MOLECULAR AND CELLULAR BIOLOGY, Apr. 2005, p. 3163–3172 Vol. 25, No. 8
0270-7306/05/$08.00+0 doi:10.1128/MCB.25.8.3163–3172.2005

Inactivation of the Arylhydrocarbon Receptor Nuclear Translocator (Arnt) Suppresses von Hippel-Lindau Disease-Associated Vascular Tumors in Mice

Erinn B. Rankin,[1,2] Debra F. Higgins,[1] Jacqueline A. Walisser,[3] Randall S. Johnson,[4] Christopher A. Bradfield,[3] and Volker H. Haase[1,2]*

Department of Medicine[1] and Cell and Molecular Biology Graduate Group, Program in Cell Growth and Cancer,[2] University of Pennsylvania School of Medicine, Philadelphia, Pennsylvania; McArdle Laboratory for Cancer Research, University of Wisconsin Medical School, Madison, Wisconsin[3]; and Molecular Biology Section, Division of Biological Sciences, University of California—San Diego, La Jolla, California[4]

Received 3 September 2004/Returned for modification 7 October 2004/Accepted 11 January 2005

Patients with germ line mutations in the *VHL* tumor suppressor gene are predisposed to the development of highly vascularized tumors within multiple tissues. Loss of pVHL results in constitutive activation of the transcription factors HIF-1 and HIF-2, whose relative contributions to the pathogenesis of the VHL phenotype have yet to be defined. In order to examine the role of HIF in von Hippel-Lindau (VHL)-associated vascular tumorigenesis, we utilized Cre-*loxP*-mediated recombination to inactivate hypoxia-inducible factor-1α (*Hif-1α*) and arylhydrocarbon receptor nuclear translocator (*Arnt*) genes in a VHL mouse model of cavernous liver hemangiomas and polycythemia. Deletion of *Hif-1α* did not affect the development of vascular tumors and polycythemia, nor did it suppress the increased expression of vascular endothelial growth factor (*Vegf*) and erythropoietin (*Epo*). In contrast, phosphoglycerokinase (*Pgk*) expression was substantially decreased, providing evidence for target gene-dependent functional redundancy between different Hif transcription factors. Inactivation of *Arnt* completely suppressed the development of hemangiomas, polycythemia, and Hif-induced gene expression. Here, we demonstrate genetically that the development of VHL-associated vascular tumors in the liver depends on functional ARNT. Furthermore, we provide evidence that individual HIF transcription factors may play distinct roles in the development of specific VHL disease manifestations.

Germ line mutations in the *VHL* tumor suppressor gene result in von Hippel-Lindau (VHL) disease, a familial tumor syndrome that predisposes affected patients to the development of highly vascularized neoplasms. These include hemangioblastomas of the retina and central nervous system (CNS), renal-cell carcinomas (RCC) of the clear-cell type, and endocrine and exocrine pancreatic tumors, as well as pheochromocytomas (34). In addition, *VHL* has also been found to be inactivated in the majority of sporadic RCC (8, 13).

VHL deficiency leads to constitutive activation of hypoxia-inducible factor (HIF) and increased expression of its target genes irrespective of the oxygen concentration (38). The *VHL* gene product (pVHL), together with elongins B and C (6, 25), Cullin-2 (43), and Rbx1 (23), forms an E3 ubiquitin ligase (19), which targets the hydroxylated, oxygen-sensitive α subunits of HIF-1, -2, and -3 for ubiquitination and subsequent degradation by the 26S proteasome (18, 20, 39). As a normal physiological response to hypoxia, HIF-1 and HIF-2 facilitate both oxygen delivery and adaptation to oxygen deprivation by regulating genes that are involved in glucose uptake and metabolism, angiogenesis, erythropoiesis, cell proliferation, and apoptosis (50, 62). HIFs belong to the PAS (Per-Arnt-Sim) family of basic helix-loop-helix (bHLH) transcription factors that bind to DNA as heterodimers composed of an oxygen-sensitive α subunit and a constitutively expressed β subunit, also known as the arylhydrocarbon receptor nuclear translocator (ARNT). ARNT is the general binding partner for the bHLH/PAS domain-containing proteins. In addition to forming heterocomplexes with HIF, ARNT also heterodimerizes with single minded (SIM), which is involved in neural development, and with the arylhydrocarbon receptor (AhR), which is involved in the xenobiotic response to environmental toxins (for a review, see reference 24).

The expression patterns of the HIF subunits differ within embryonic and adult tissues. In the adult, *Hif-1α* mRNA is ubiquitously expressed, and Hif-1α protein can be detected at baseline levels within multiple cell types in various tissues under normoxia and is significantly enhanced under conditions of hypoxia (55). In contrast, while *Hif-2α* mRNA expression has been detected within many tissues, Hif-2α protein has been found to be restricted to specific cell types within various tissues. In addition to being expressed in endothelial cells, *Hif-2α* is also expressed in glial cells of the brain, type II pneumocytes of the lung, cardiomyocytes, fibroblasts of the kidney, intersitial cells of the pancreas and duodenum, and hepatocytes (26, 63). *Arnt* expression is ubiquitous, and it seems to be the only Hif-β subunit present in the liver (21).

pVHL appears to have multiple functions besides regulating HIF, and its contributions to the development of VHL-associated tumors are presently subject to intense investigations. As a result of these efforts, it has been shown that pVHL plays an important role in fibronectin extracellular-matrix assembly (41) and microtubule stabilization (12). The importance of

* Corresponding author. Mailing address: Department of Medicine, 700 Clinical Research Bldg., 415 Curie Blvd., Philadelphia, PA 19104-6144. Phone: (215) 573-1830. Fax: (215) 898-0189. E-mail: vhaase@mail.med.upenn.edu.

proper pVHL function during development and in the adult is illustrated by the fact that homozygous deletion of the murine *Vhl* gene (*Vhlh*) results in embryonic lethality. Mice homozygously deficient in *Vhlh* die in utero between embryonic days 10.5 and 12 due to a defect in embryonic vasculogenesis of the placenta (9). We and others have previously shown that mice with a heterozygous germ line deletion of *Vhlh* have a predisposition to develop cavernous hemangiomas of the liver (10, 32). These hepatic vascular tumors display some of the histological features observed in VHL hemangioblastomas, which can also be found at low frequency in the livers of patients with VHL disease (10). Tissue-specific deletion of floxed *Vhlh* via Albumin-Cre mediated recombination in hepatocytes recapitulated the vascular phenotype found in *Vhlh* heterozygotes and suggested that loss of pVhl function in hepatocytes was responsible for the development of vascular tumors (10).

In order to examine the role of HIF in the development of VHL-associated vascular tumors, we utilized Cre-*loxP*-mediated recombination to inactivate either Hif-1α or Arnt in *Vhlh*-deficient hepatocytes. In this report, we show that loss of Arnt is sufficient to suppress the development of liver hemangiomas and erythrocytosis in *Vhlh* mutant mice, while loss of Hif-1α is not. We also provide evidence that in regard to HIF-regulated gene expression, target gene-dependent functional redundancy exists between different HIF homologues. Based on our data, we propose that in patients, the development of VHL-associated hemangiomas is mediated by increased HIF transcriptional activity and that the different HIF homologues may play distinct roles in the development of certain clinical features associated with VHL disease.

MATERIALS AND METHODS

Generation and genotyping of mice. The generation of mice carrying the *Vhlh*, *Hif-1*α *2-lox*, and *Arnt 3-lox* alleles and the *Albumin-Cre* transgenes has been described (10, 45, 48). Phosphoenolpyruvate carboxykinase-Cre (PEPCK-Cre) transgenic mice were generated by targeted single-copy transgenesis in embryonic stem cells (Rankin and Haase, unpublished data). Mutant mice were in a mixed genetic background (BALB/c, 129Sv/J, and C57BL/6). All procedures involving mice were performed in accordance with the National Institutes of Health guidelines for the use and care of live animals and were approved by the University of Pennsylvania Institutional Animal Care and Use Committee.

The following primers were used to detect 2-*lox*, 1-*lox*, and wild-type alleles of *Vhlh*: FwdI (5′-CTGGTACCCACGAAACTGTC-3′), FwdII (5′-CTAGGCACC GAGCTTAGAGGTTTGCG-3′), and Rev (5′-CTGACTTCCACTGATGCTT GTCACAG-3′). The *Vhlh* 2-*lox* allele was identified by the 460-bp band, the 1-*lox* allele was identified by a 260-bp band, and the wild-type allele was identified as a 290-bp band. The *Hif1*-α 2-*lox*, 1-*lox*, and wild-type alleles were detected with the following primers: FwdI (5′-TTGGGGATGAAAACATCTGC-3′), FwdII (5′-GCAGTTAAGAGCACTAGTTG-3′), and Rev (5′-GGAGCTATCTCTCT AGACC-3′). The *Hif-1*α 1-*lox* allele was identified as a 270-bp band, the 2-*lox* allele was identified as a 260-bp band, and the wild-type allele was identified as a 240-bp band. The *Arnt* 3-*lox*, 1-*lox*, and wild-type alleles were identified with the following primers: Fwd (5′-GCAACTTTGACAAGGCAGCATTTA-3′), RevI (5′-GGCAGGGGGAATCTCTGAGTTCT-3′), and RevII (5′-ACACCCTTCT TTCACTTCACAG-3′). The 1-*lox* allele band was identified as a 400-bp band, the 3-*lox* allele was identified as a 174 bp, and the wild-type allele was identified as a 140-bp band.

DNA and RNA isolation. Mouse tail DNA was isolated according to the method of Laird et al. (31) and was used for genomic PCR. DNA and RNA from mouse livers were isolated using Trizol reagent (Invitrogen) according to the manufacturer's guidelines.

Protein preparation and immunoblot analysis. Cytoplasmic and nuclear protein fractions were isolated using the protocol described by Camenisch et al. (1). Mouse liver was homogenized and lysed in buffer A. Cytoplasmic protein fractions were collected, and nuclei were lysed in buffer C to obtain nuclear protein extracts. Nuclear proteins were then dialyzed twice for 2 h each time at 4°C in buffer D. Protein concentrations were determined using the Bio-Rad Protein Assay. Twenty micrograms of each protein extract was size separated by 3 to 8% gradient sodium dodecyl sulfate-polyacrylamide gel electrophoresis (Invitrogen) and transferred to nitrocellulose membranes (Amersham Pharmacia Biotech). The membranes were stained with Ponceau S solution (Sigma) to determine equal protein loading. After being blocked in 10% nonfat dry milk (Carnation)–Tris-buffered saline–Tween 20 solution, the blots were incubated with 5% nonfat dry milk–Tris-buffered saline–Tween 20 solutions containing rabbit anti-mouse Hif-2α (raised against amino acids 580 to 693) or monoclonal Hif-1α (Novus Biologicals). The blots were then washed and incubated with horseradish peroxidase-conjugated goat anti-rabbit (Bio-Rad Laboratories) or sheep anti-mouse (Amersham Pharmacia Biotech) secondary antibodies according to the manufacturers' instructions. Enhanced chemiluminescence reagents obtained from Amersham Pharmacia Biotech were used as a detection system according to the manufacturer's instructions. Blots were stripped in a 2× 7 M guanidine HCl–50 mM Tris-HCl (pH 7.4) solution for 30 min at room temperature, followed by a 1× solution for 30 min, before being blocked and reprobed.

Gel shift. Nuclear proteins were isolated, and an electrophoretic mobility shift assay (EMSA) was performed using the erythropoietin (*Epo*) hypoxia response element (HRE) as previously described (1). The Epo sense oligonucleotide 5′-GCCCTACGTGCTGTCTCACACAGC-3′ was annealed to the antisense oligonucleotide 5′-GCTGTGTGAACAGCACGTA-3′ in 1× annealing buffer containing 10 mM Tris-Cl (pH 7.8) and 50 mM NaCl by heating them to 95°C for 3 min and slowly cooling them to room temperature. Similarly, the *AP-1* competitor sense (5′-TTCCGGCTGACTCATCAAGCG-3′) and antisense (5′-CGCTT GATGAGTCAGCCGGAA-3′) oligonucleotides were annealed together. The annealed *Epo* oligonucleotides were then labeled with 50 μCi of α-dCTP and α-dGTP (Amersham) using Klenow (Promega). The labeled oligonucleotides were then run through a G-50 microcolumn (Amersham), counted on a scintillation counter, and diluted to 30,000 cpm/μl in Tris-EDTA buffer. Protein binding reactions and electrophoresis were performed as previously described (Camenisch et al. [1]). Supershift reactions were performed using either monoclonal Hif-1α (Novus Biologicals) or monoclonal Hif-2α (Novus Biologicals) antibody and were incubated with the protein AP-1 (activator protein 1) competitor oligonucleotide and probe for 2 h at 4°C prior to electrophoresis.

Blood and histological analysis. For the determination of the blood hemoglobin (Hgb) concentration and red blood cell (RBC) numbers, blood was collected and analyzed with a Hemavet 1500 CBC analyzer (CDC Technologies). For histological analysis, tissues were fixed in 10% phosphate-buffered formalin overnight at 4°C and processed for routine embedding in paraffin. Sections of 6-μm thickness were stained with hematoxylin and eosin using standard staining procedures. LacZ staining was performed on tissue sections frozen in optical cutting temperature (OCT; Tissue-Tek) according to the method of MacGregor et al. (33).

Reverse transcription-PCR. cDNA was synthesized from 4 μg of DNase (Invitrogen)-treated RNA isolated from mouse liver using the SuperScript first-strand synthesis system for reverse transcription-PCR (Invitrogen). One microliter of cDNA was subjected to PCR amplification using either SYBR GREEN PCR Master Mix or *Taq*man Universal PCR Master Mix (Applied Biosystems). The following primer and probe sets were used to amplify specific target genes: SYBR GREEN primers, *Vhlh* (Fwd, 5′-GCCTATTTTTGCCAACATCACA-3′; Rev, 5′-TCATTCTCTCTATGTGCTGGCTTT-3′), *Hif-1*α (Fwd, 5′-CAAGAT CTCGGCGAAGCAA-3′; Rev, 5′-GGTGAGCCTCATAACAGAAGCTTT-3′), *Hif-2*α, Fwd (5′-CAACCTGCAGCCTCAGTGTATC-3′; Rev, 5′-CACCAC GTCGTTCTTCTCGAT-3′), VegfA (Fwd, 5′-CCACGTCAGAGAGCAACAT CA-3′; Rev, 5′-TCATTCTCTCTATGTGCTGGCTTT-3′), *Epo* (Fwd, 5′-CATC TGCGACAGTCGAGTTCTG-3′; Rev, 5′-CACAACCCATCGTGACATTTT C-3′), *Bnip3* (Fwd, 5′-GACGAAGTAGCTCCAAGAGTTCTCA-3′; Rev, 5′-C TATTTCAGCTCTGTTGGTATCTTGTG-3′), *Pgk* (Fwd, 5′-GGAAGCGGGT CGTGATGA-3′; Rev, 5′-GCCTTGATCCTTTGGTTGTTTG-3′; Taqman primers and probes, *18S* (Human 18S rRNA Taqman set [Applied Biosystems]), *Arnt* (Fwd, 5′-CGAAAACCAGACAAGCTAACCA-3′; Rev, 5′-TGTTGCCAG TTCCCCTCAAG-3′; Probe, 5′-CTTACGCATGGCCGTTTCTCACATGAA-3′). PCR amplification was performed on the Prism 7700 Sequence Detection System (Applied Biosystems). The thermal-cycling profile used was denaturation at 50°C for 2 min and 95°C for 10 min, followed by cycles of denaturation at 95°C for 15 s and 60°C for 1 min. *18S* was used to normalize mRNA. Relative quantitation of mRNA expression levels was determined using the relative standard curve method according to the manufacturer's instructions (Applied Biosystems).

Statistical analysis. For statistical analysis and comparison of numbers of liver hemangiomas in *Vhlh* and *Vhlh*/*Hif-1*α mutant mice, the chi-square test was

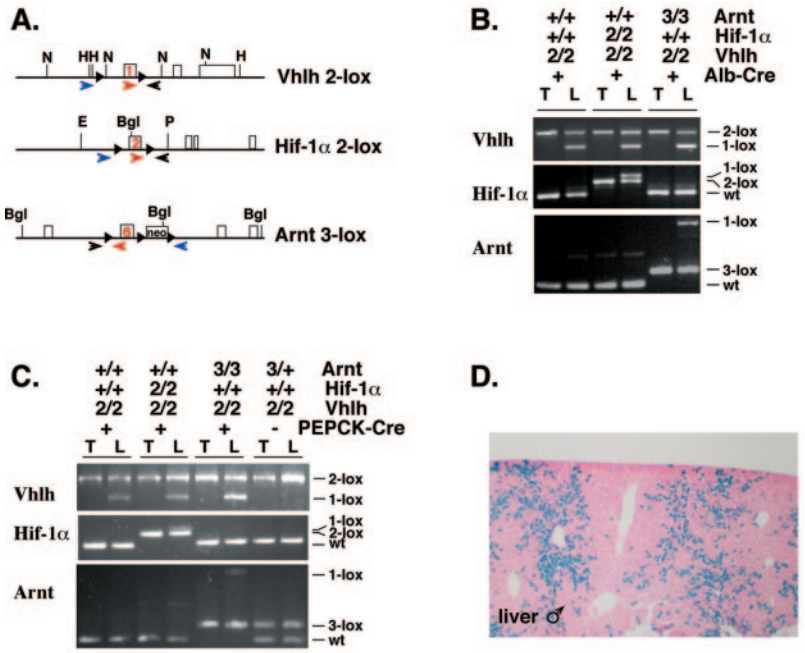

FIG. 1. Generation of mice deficient for *Vhlh*, *Vhlh*/*Hif-1*α, and *Vhlh*/*Arnt* in hepatocytes. (A) Genomic maps for the targeted *Vhlh* 2-*lox*, *Hif-1*α 2-*lox*, and *Arnt* 3-*lox* alleles. Exons are depicted as rectangular boxes with the *loxP* floxed exon numbered. *loxP* sites are represented by black triangles. The locations of primers used for genomic PCR are shown with colored arrows. All three primers were used in a single PCR to specifically amplify the nonrecombined conditional allele (2-*lox*) or wild type with the red and black primers and the recombined allele (1-*lox*) with the blue and black primers. Genomic maps are not complete or drawn to scale. Abbreviations: neo, neomycin selection marker; H, HindIII; N, NcoI; E, EcoRI; P, PstI; Bgl, BglII. (B) Genotype analysis of Albumin-Cre mutant mice by genomic PCR. Abbreviations: 2, 2-*lox*; 3, 3-*lox*; +, wild type (wt) (+ for Alb-Cre indicates the presence of the *Albumin-Cre* transgene); T, tail; L, liver. (C) Genotype analysis of PEPCK-Cre mutant mice by genomic PCR. (D) Qualitative analysis of PEPCK-Cre expression in the liver. LacZ staining of a liver section collected from a male PEPCK-Cre mouse crossed with the ROSA26 LacZ reporter mouse (52). Blue staining indicates hepatocytes that have undergone Cre-mediated recombination.

performed. For statistical analysis of gene expression data, red blood cell numbers, and hemoglobin concentrations, analysis of variance, followed by the unpaired Student's *t* test, was performed. *P* values of <0.05 were considered statistically significant.

RESULTS

Efficient deletion of *Hif-1*α and *Arnt* in *Vhlh*-deficient hepatocytes. We have previously reported that mice that are heterozygously deficient for *Vhlh* are predisposed to develop cavernous hemangiomas of the liver with high phenotypical penetrance at old age (10). Vascular lesions can be reproduced by Cre-mediated recombination of a *Vhlh* conditional allele (2-*lox* allele) in hepatocytes (10). To examine the requirement for HIF in VHL-associated vascular tumorigenesis, we used two Cre-transgenic lines, Albumin-Cre (45) and PEPCK-Cre, to inactivate both *Vhlh* and *Hif-1*α or *Vhlh* and *Arnt* in hepatocytes. In the *Vhlh* conditional allele, deletion of exon 1 and the promoter by Cre-mediated recombination results in a *Vhlh* null allele (1-*lox* allele) (Fig. 1A) (10). In the *Hif-1*α and *Arnt* conditional alleles, *Hif-1*α exon 2 and *Arnt* exon 6, which both encode the bHLH domain, undergo Cre-mediated out-of-frame deletion, resulting in the absence of Hif-1α or Arnt (Fig. 1A) (48, 60). Inactivation of *Hif-1*α results in the inability to form functional Hif-1, while it does not affect the formation of Hif-2 heterocomplexes (48, 53), whereas inactivation of *Arnt* prevents the formation of functional Hif-1 and Hif-2, but not nuclear translocation of Hif-α homologues (2).

It has been reported that Albumin-Cre is active in >80% of hepatocytes and recombines floxed alleles with high efficiency (45). High-efficiency gene deletion in Albumin-Cre mutants (*Vhlh*$^{2lox/2lox}$, *Hif-1*α$^{2lox/2lox}$; *Albumin-Cre* or *Vhlh3*$^{2lox/2lox}$, *Arnt*$^{3lox/3lox}$; *Albumin-Cre* [referred to hereafter as *Albumin-Vhlh*/*Hif-1*α or *Albumin-Vhlh*/*Arnt* double mutants]) is shown in Fig. 1B and is consistent with previously reported findings (10). Since Albumin-Cre-mediated inactivation of *Vhlh* results in relatively complex liver pathology, which includes an increase in nonhepatocyte cell types, such as endothelial cells (10), genomic PCR of DNA isolated from whole livers most likely underestimates recombination efficiency in *Albumin-Vhlh* and *Vhlh*/*Hif-1*α livers. Recombination efficiency is therefore best assessed in *Vhlh*/*Arnt* double mutants, which have histologically normal livers (Fig. 1B; also see Fig. 3). Due to the high degree of Cre-mediated recombination in these mice, Albumin-Cre mutant mice were used for gene expression studies. Albumin-Cre-mediated targeting of *Vhlh* results in severe hepatic steatosis (neutral fat accumulation in hepatocytes) and angiectasis. Mutant mice died at an early age (10), thus precluding long-term studies of adult mice.

In contrast to Albumin-Cre mutants, PEPCK-Cre *Vhlh* mutants lived to at least 15 months of age and developed cavernous liver hemangiomas (Fig. 2A). In the *PEPCK-Cre* transgene *Cre-recombinase* is under the control of the rat *PEPCK* promoter (42). The *PEPCK-Cre* transgene was generated by targeted single-copy transgenesis in embryonic stem cells and is

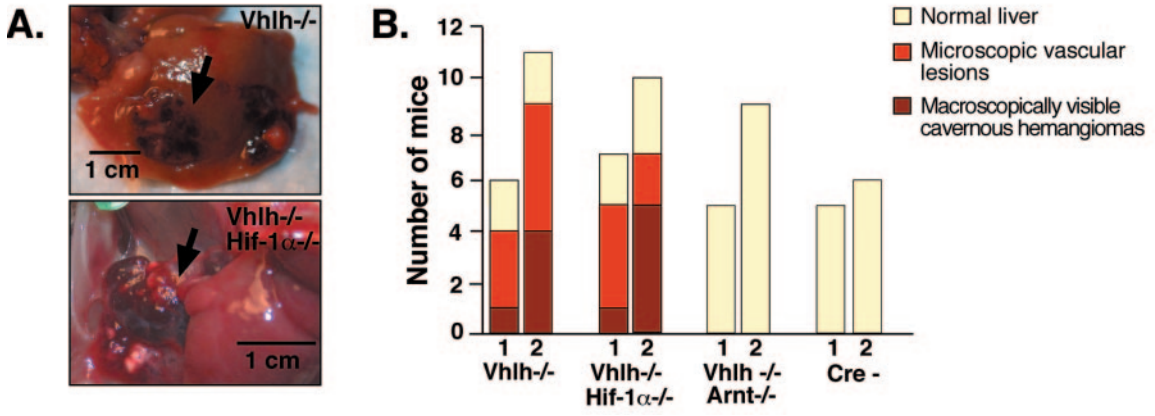

FIG. 2. Inhibition of vascular-tumor development in *Vhlh*/*Arnt* mutant mice. (A) Photographs of gross cavernous liver hemangiomas observed in *PEPCK-Vhlh* and *PEPCK-Vhlh*/*Hif-1*α mutant mice. Hemangiomas are indicated by arrows. (B) Incidence of macroscopic liver hemangiomas and microscopic vascular lesions observed in PEPCK-Cre mutant mice. Mice from the indicated genotypes were divided into two age groups for analysis, mice 2 to 6 months of age (group 1) and mice >6 months of age (group 2). Each bar represents the number of mice from the indicated genotype with macroscopic hemangiomas, microscopic vascular lesions in the liver, and normal liver. A chi-square test revealed that there were no significant differences between the distributions of macroscopic and microscopic liver hemangiomas in the *Vhlh*- and *Vhlh*/*Hif-1*α-deficient mice.

located on the X chromosome upstream of the hypoxanthine-phosphoribosyltransferase (*Hprt*) gene (E. B. Rankin and V. H. Haase, unpublished data). Since *PEPCK-Cre* is located on the X chromosome, it is most likely subject to random X chromosome inactivation (for a review, see reference 4); we observed variable recombination efficiency in female mice that were heterozygous for the transgene (data not shown). In order to reduce experimental variability, the majority of mice used for analysis of the PEPCK mutant phenotype were male mice.

To determine the requirement for Hif-1α and Arnt in the development of VHL-associated liver hemangiomas, we generated mice that were made double deficient for either *Vhlh* and *Hif-1*α or *Vhlh* and *Arnt* by PEPCK-Cre-mediated recombination. For this purpose, *PEPCK-Cre* transgenic mice were bred to mice that were homozygous for either *Vhlh* (10) and *Hif-1*α (48) or *Vhlh* and *Arnt* (60) conditional alleles to generate double-mutant mice: $Vhlh^{2lox/2lox}$, $Hif\text{-}1\alpha^{2lox/2lox}$; *PEPCK-Cre* or $Vhlh^{2lox/2lox}$, $Arnt^{3lox/3lox}$; *PEPCK-Cre* (hereafter referred to as either *PEPCK-Vhlh*/*Hif-1*α or *PEPCK-Vhlh*/*Arnt* double mutants). PEPCK-Cre-mediated recombination efficiency was examined by genomic PCR and with the ROSA26 LacZ reporter (Fig. 1C and D) (52). Consistent with the expression pattern of the endogenous gene (42), PEPCK-Cre was found to be active in ~20 to 30% of hepatocytes. Genomic PCR results were found to be comparable with the results from the ROSA26 Cre reporter study (Fig. 1C and D).

Inactivation of *Arnt* is required to suppress the development of liver hemangiomas in *Vhlh* mutants. To determine the requirement for *Hif-1*α and *Arnt* in the development of liver hemangiomas, we examined the livers of *PEPCK-Vhlh*/*Hif-1*α and *PEPCK-Vhlh*/*Arnt* double-mutant mice macroscopically and histologically. Mice were divided into two age groups, 2 to 6 months of age (group 1) and >6 months of age (group 2). The oldest mice analyzed were 15 months of age. We observed that, similar to *PEPCK-Vhlh* mutants, 6 of 17 *Vhlh*/*Hif-1*α double mutants developed large cavernous hemangiomas compared to 5 of 17 *PEPCK-Vhlh* mutants, resulting in no significant difference in the number of hemangiomas that developed between the two mutants, as determined by the chi-square test ($P = 0.71$) (Fig. 2A and B). Although the number of large cavernous hemangiomas per individual liver was usually limited to <5, we observed focal microscopic changes throughout the liver that were similar to those previously reported for *Vhlh* heterozygotes and Albumin-Cre mutants (10). Typically, those microscopic vascular lesions consisted of hepatocellular steatosis, angiectasis, and endothelial cell proliferation (Fig. 3). The frequencies of mice that exhibited only focal microscopic lesions were similar for the *Vhlh* single mutant (8 of 17) and for the *Vhlh*/*Hif-1*α double mutant (6 of 17). Strikingly, we did not observe any of the same lesions (microscopic or macroscopic) in *PEPCK-Vhlh*/*Arnt* livers, which at an early age were histologically identical to control livers (Fig. 2B). Moderate steatosis without angiectasis or cellular proliferation was found in *Vhlh*/*Arnt* double mutants (three of nine) at older ages (>9 months), which may be a result of the inability to form Hif-2 heterodimers, as hepatic steatosis has been reported in Hif-2α germ line knockout mice (49).

Similar to PEPCK mutants, *Albumin-Vhlh* single mutants did not differ significantly from *Albumin-Vhlh*/*Hif-1*α double mutants and developed severe hepatic steatosis associated with angiectasis and endothelial cell proliferation, as previously reported (10). *Albumin-Vhlh*/*Arnt* double mutants appeared histologically normal at the age used for this study (4 to 6 weeks of age) (Fig. 3). We conclude from our data that the inability to generate transcriptionally active Hif-1 is not sufficient to prevent the development of VHL-associated vascular tumors and that inactivation of Arnt is sufficient to suppress the VHL phenotype in mice.

Inactivation of *Hif-1*α is not sufficient to suppress the development of VHL-associated polycythemia. A subset of VHL patients with renal cell carcinoma and capillary hemangioblastomas develop polycythemia, which correlates with upregulation of *Epo* expression in tumors (5, 30). *Epo* is a classic

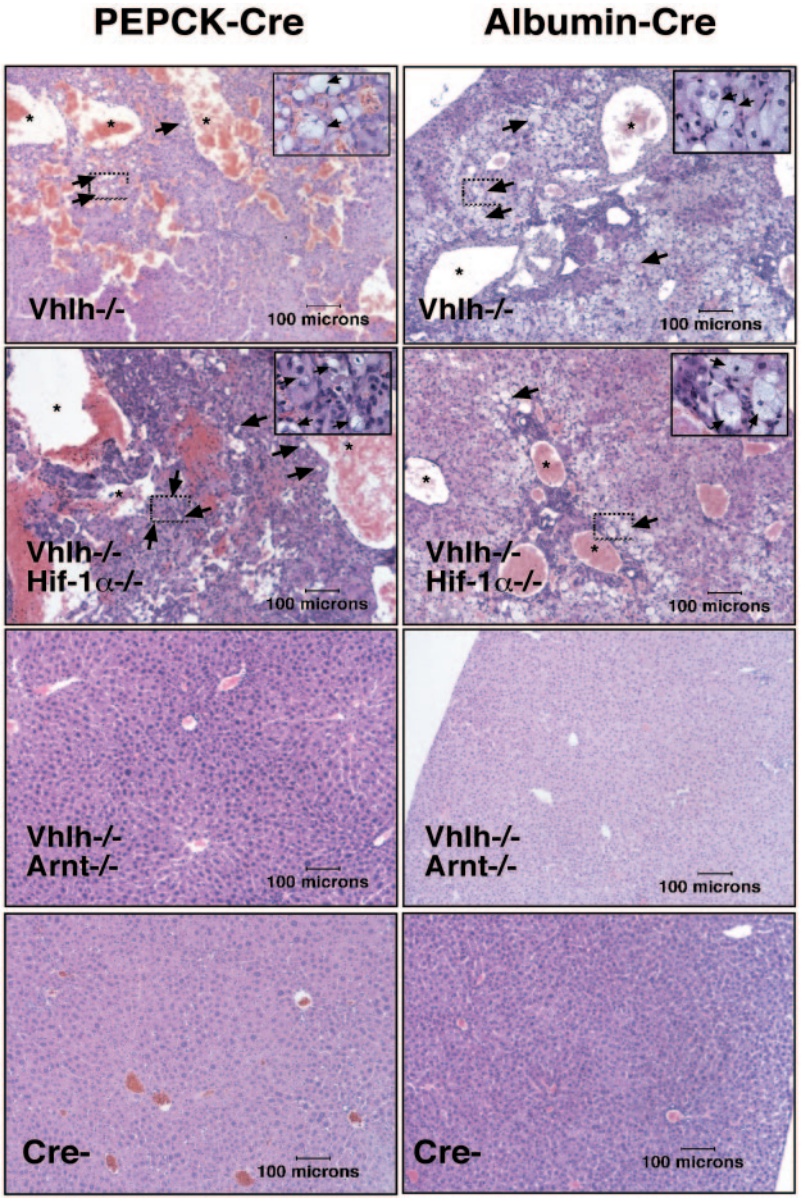

FIG. 3. Inactivation of *Arnt* suppresses *Vhlh*-associated vascular lesions and steatosis. Hematoxylin and eosin staining of PEPCK-Cre (left; >6 months of age) and Albumin-Cre (right; 4 to 6 weeks of age) mutant liver sections (magnification, ×100). Note that large vascular spaces (stars) and steatosis (arrows) were observed in both *Vhlh* and *Vhlh*/*Hif-1*α mutant mice. The black boxes outline areas that are shown at higher magnification (×1,000) in the upper right corners.

hypoxia-inducible gene, and investigations aimed at the identification of transcription factors responsible for hypoxic induction of *Epo* mRNA eventually led to the purification of HIF-1 (for a review, see reference 51). We previously reported that inactivation of *Vhlh* in the mouse liver also results in polycythemia as a result of increased serum Epo levels (10). Similarly, we observed that *PEPCK-Vhlh* mutant mice developed erythrocytosis that clinically manifested as redness of the paws and muzzle (Fig. 4A). To determine whether the development of VHL-associated erythrocytosis was exclusively dependent on increased Hif-1 transcriptional activity, we compared RBC numbers and total Hgb concentrations in *PEPCK-Vhlh* mutants to those in *PEPCK-Vhlh*/*Hif-1*α and *PEPCK-Vhlh*/*Arnt* mice. We found that *PEPCK-Vhlh*- and *Vhlh*/*Hif-1*α-deficient mice developed similar degrees of erythrocytosis, with average RBC counts and Hgb values of $11.17 \times 10^6 \pm 0.9 \times 10^6/mm^3$ and 20.05 ± 2.81 g/dl for *Vhlh* mutants and $10.77 \times 10^6 \pm 1.22 \times 10^6/mm^3$ and 19.38 ± 1.76 g/dl for *Vhlh*/*Hif-1*α double mutants ($n = 6$ in all groups). In contrast, *Vhlh*/*Arnt* double-mutant mice had normal RBC counts, with average RBC numbers and Hgb values of $8.21 \times 10^6 \pm 0.82 \times 10^6/mm^3$ and 12.8 ± 0.635 g/dl, respectively, compared to values of $9.3 \times 10^6 \pm 0.62 \times 10^6/mm^3$ and 13.24 ± 0.48 g/dl in control mice (Fig. 4B).

To determine if erythrocytosis correlated with increased *Epo* expression, we measured *Epo* mRNA levels in whole-liver homogenates. *PEPCK-Vhlh* and *PEPCK-Vhlh*/*Hif-1*α mice exhib-

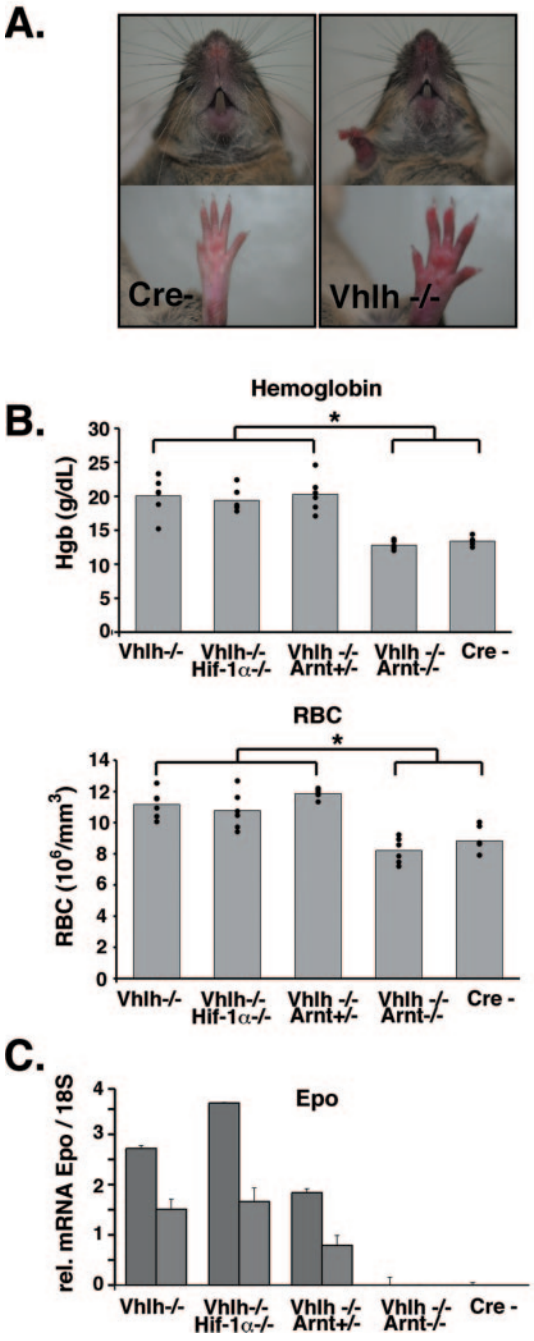

FIG. 4. Inactivation of *Vhlh* and *Vhlh*/*Hif-1*α in hepatocytes induces erythrocytosis. (A) Control (Cre$^-$) and *PEPCK-Vhlh* muzzles and paws. Note the increased red coloration of the skin in the *PEPCK-Vhlh* mutant mouse. (B) Elevated hemoglobin and red blood cell numbers in *PEPCK-Vhlh*- and *PEPCK-Vhlh*/*Hif-1*α-deficient mutant mice. The results shown are average hemoglobin concentrations and RBC numbers in blood collected from PEPCK-Cre mutant mice determined by a CBC analyzer. Note that *Vhlh*/*Arnt* mutant mice and control mice have similar hemoglobin concentrations and red blood cell numbers (no statistical differences as determined by *t* test). *Vhlh*-, $Vhlh^{-/-}/Hif\text{-}1\alpha^{-/-}$, and $Vhlh^{-/-}/Arnt^{+/-}$ mice exhibited increased levels of hemoglobin and red blood cells compared to control and $Vhlh^{-/-}/Arnt^{-/-}$ mice (*, $P < 0.05$). Six mice from each genotype were analyzed and are represented by individual dots. (C) Liver erythropoietin expression correlates with erythrocytosis. Shown are *Epo* mRNA expression levels from PEPCK-Cre mutant livers determined by real-time PCR. Each bar represents the average of three values obtained for an individual mouse. The error bars represent standard deviations. *18S* was used to normalize mRNA. Two representative mice from an *n* of 3 are shown for each genotype.

ited increased *Epo* mRNA expression, whereas *PEPCK-Vhlh*/*Arnt* and control mice did not express detectable levels of *Epo* mRNA transcripts, as determined by real-time PCR (Fig. 4C). We conclude that increased production of *Epo* in *Vhlh*-deficient livers is not dependent on Hif-1, suggesting that loss of Hif-1 can be compensated for by other Hif heterocomplexes.

Differential suppression of Hif target genes in *Vhlh*/*Hif-1*α double-mutant mice. The liver expresses at least two Hif homologues that have been shown to function as hypoxia-responsive transcriptional activators, namely, Hif-1 and Hif-2 (26, 55, 63). In order to determine to what degree Hif target gene expression in the liver is Hif-1 dependent, we examined *Vegf*, *Epo*, phosphoglycerokinase (*Pgk*), and *Bnip3* mRNA levels in wild-type and *Vhlh*-, *Vhlh*/*Hif-1*α-, and *Vhlh*/*Arnt*-deficient livers. For these studies, we analyzed Albumin-Cre mutants due to the limited expression of PEPCK-Cre in the liver. We first determined mRNA expression levels for the *loxP* targeted genes in each of the mice analyzed. Real-time PCR analysis revealed a robust reduction of *Hif-1*α and *Arnt* mRNA expression in all Albumin-Cre mutant mice homozygous for the *Hif-1*α (groups 2 and 5) or *Arnt* (groups 4 and 6) floxed alleles (Fig. 5A). Reduction of *Vhlh* mRNA in whole-liver homogenates from *Vhlh* mutants (Fig. 5A, group 1) was less pronounced, probably due to the presence of nonrecombined cells, such as proliferating endothelial and other nonhepatocyte cell types (Fig. 3), which also may have resulted in a relative increase in *Hif-1*α and *Arnt* mRNA levels. Consistent with the increased presence of the *Vhlh* 1-*lox* allele (Fig. 1B) is the reduction of *Vhlh* mRNA levels by ~75% in *Vhlh*/*Arnt* double mutants (Fig. 5A, group 4). In addition, we determined the relative expression levels of *Hif-2*α in the Albumin-Cre mutant livers. We observed that, similar to *Arnt*, expression of *Hif-2*α was significantly increased in *Vhlh* and *Vhlh*/*Hif-1*α mutants ($P < 0.001$; groups 1 and 2). This may be either a result of *Vhlh* deletion, as induction of *HIF-2*α mRNA expression in *VHL*-deficient renal cell carcinoma cells has been described (29), or the result of the increased presence of nonrecombined cells.

Real-time PCR analysis of HIF target genes revealed that mRNA transcripts for *Vegf* and *Epo* were increased in both *Vhlh*- and *Vhlh*/*Hif-1*α-deficient livers, whereas *Vhlh*/*Arnt* double-mutant livers expressed transcript levels comparable to those in control mice (Fig. 5B). Similarly, *Pgk* and *Bnip3* mRNA transcripts were increased in *Vhlh*- and *Vhlh*/*Hif-1*α-deficient livers and were expressed at baseline levels in the *Vhlh*/*Arnt* mutant livers. However, expression levels of *Pgk* in *Vhlh*/*Hif-1*α double mutants were significantly reduced compared to those in *Vhlh* mutants ($P < 0.01$), while *Bnip3* mRNA levels were less affected (Fig. 5B). These results suggest that the functional redundancy between different Hif transcription factors is target gene dependent. The inability to form Hif-1 heterodimers had little effect on *Vegf* and *Epo* gene expression, which is consistent with the persistence of excessive erythrocytosis in *Vhlh*/*Hif-1*α double mutants and their predisposition to

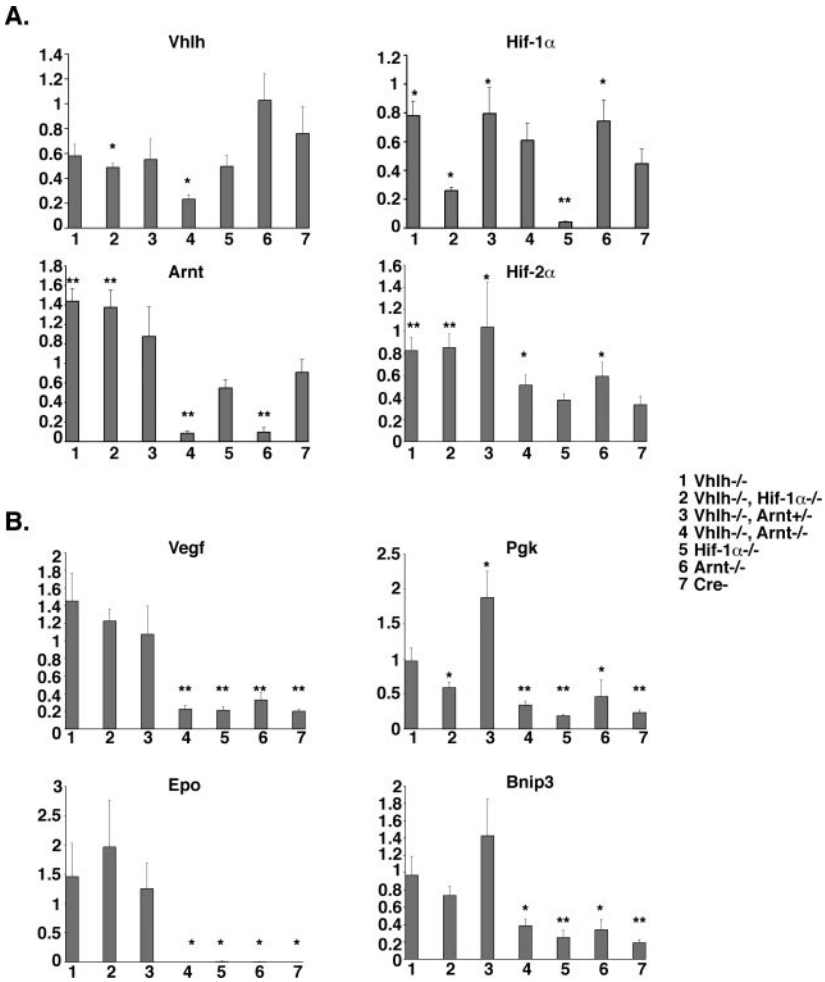

FIG. 5. Inactivation of *Arnt* is sufficient to suppress Hif target gene induction in *Vhlh*-deficient livers. (A) Suppression of targeted gene (*Vhlh*, *Hif-1*α, and *Arnt*) expression in Albumin-Cre mutant livers. Shown are relative mRNA transcript levels normalized to *18S* levels determined by real-time PCR. Note that Albumin-Cre-mediated inactivation of *Vhlh* is best represented in the *Vhlh*/*Arnt* double-mutant mice. Each bar represents the average mRNA expression level of four individual mice for each genotype. The error bars represent the standard deviations. Asterisks indicate a significant increase or decrease in target gene expression compared to control mice (Cre^-) (*, $P < 0.05$; **, $P < 0.001$) as determined by the *t* test. (B) Relative mRNA expression levels for HIF target genes (*Vegf*, *Epo*, *Pgk*, and *Bnip3*) determined by real-time PCR. Each bar represents the average mRNA expression level of four individual mice for each genotype. The error bars represent standard deviations. Asterisks indicate a significant increase or decrease in target gene expression compared to $Vhlh^{-}/^{-}$ mice (*, $P < 0.05$; **, $P < 0.001$) as determined by the *t* test. 18S was used to normalize mRNA.

the development of vascular tumors. Our data demonstrate that inactivation of Arnt is sufficient to suppress Hif target gene induction in *Vhlh*-deficient livers and suggest that another Arnt binding partner is responsible for *Vegf* and *Epo* target gene induction in *Vhlh*-deficient livers.

Hif target gene expression data from *Vhlh*/*Hif-1*α double-deficient mice suggest that Hif-2 is transcriptionally active in hepatocytes. To examine Hif-2α protein levels and nuclear localization, we performed immunoblot analysis on nuclear protein fractions isolated from Albumin-Cre mutants. Nuclear Hif-2α, as well as Hif-1α, was easily detectable in livers from *Vhlh* and *Vhlh*/*Arnt* mutants, while only Hif-2α was easily detectable in *Vhlh*/*Hif-1*α mutants (Fig. 6A). In addition, we found that both Hif-1 and Hif-2 complexes bound to the *Epo* HRE in *Vhlh*-deficient livers, whereas only Hif-2 heterocomplexes were detected in *Vhlh*/*Hif-1*α-deficient livers (Fig. 6B). Neither Hif-1α- nor Hif-2α-containing complexes were bound to the *Epo* HRE in the *Vhlh*/*Arnt* and control livers. Taken together, our data suggest that in *Vhlh*-deficient livers, Hif-2α is able to translocate to the nucleus, where it is transcriptionally active only when Arnt is present. These data are consistent with the observation that Arnt is the only Hif-β subunit expressed in the liver at significant levels (21).

DISCUSSION

In this report, we have used a conditional knockout mouse model of VHL-associated vascular tumors and erythrocytosis to investigate the contributions of HIF hetercomplexes to the development of the VHL phenotype. Typically, patients with VHL disease suffer from a variety of highly vascularized tumors, which include retinal and CNS hemangioblastomas, as

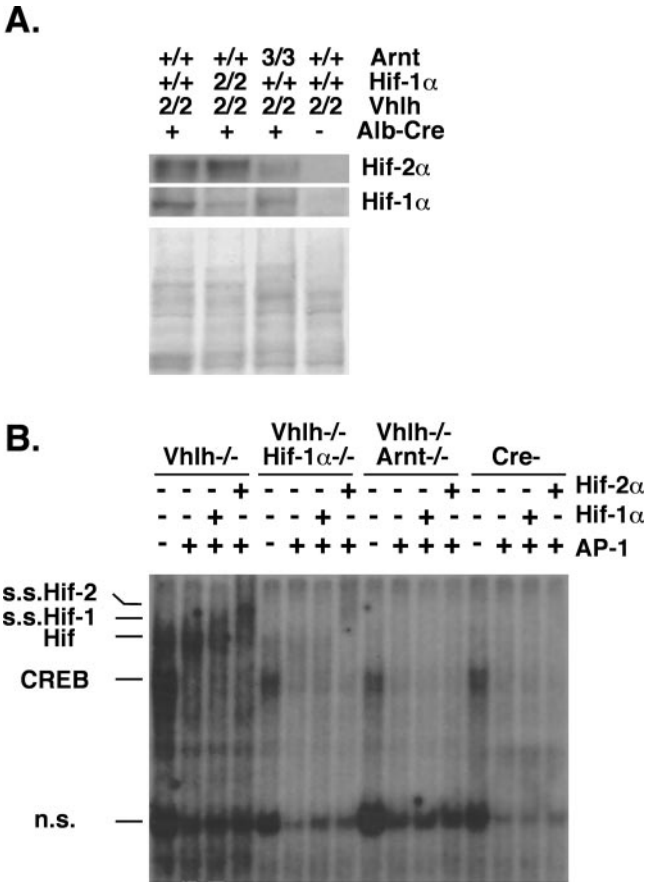

FIG. 6. Hif-2α protein stabilization and HRE binding in *Vhlh*-deficient livers. (A) Nuclear protein (N) extracts were isolated from livers of *Albumin-Vhlh*, *Albumin-Vhlh/Hif-1α*, and *Albumin-Vhlh/Arnt* mutant and control mice (Cre^-). Immunoblot analysis for Hif-2α revealed that Hif-2α protein was stable and nuclear in all *Vhlh*-deficient livers. Hif-1α protein was also detectable above baseline levels in *Vhlh*- and *Vhlh/Arnt*-deficient livers. Ponceau S staining is shown to demonstrate equal protein loading. Abbreviations: 2, 2-*lox*; 3, 3-*lox*; +, wild type (+ or − for Alb-Cre indicates the presence or absence of the *Albumin-Cre* transgene). (B) Hif-1 and Hif-2 HRE binding activity by EMSA. Nuclear protein extracts isolated from *Albumin-Vhlh*, *Vhlh/Hif-1α*, *Vhlh/Arnt*, and Cre^- livers were tested for Hif binding to the *Epo* HRE in vitro by EMSA. Supershifts with Hif-1α and Hif-2α antibodies revealed that both Hif-1 and Hif-2 form heterocomplexes at the *Epo* HRE in *Vhlh*-deficient livers. Note that Hif-2 binding to the *Epo* HRE was still observed in *Albumin-Vhlh/Hif-1α* nuclear extracts despite a decrease in total Hif HRE binding. Abbreviations: n.s., nonspecific; s.s., supershift; CREB, cAMP response element binding protein.

well as RCC of the clear-cell type (for a review, see reference 34). While the biological behaviors of these tumors are very different—hemangioblastomas are usually benign and do not metastasize, whereas RCC are malignant—they share several molecular features. In both cases, mutant pVHL lacks the ability to target HIF for proteasomal degradation, resulting in constitutively active HIF (3, 15). VHL tumors express high levels of HIF target genes that regulate angiogenic growth factors, such as VEGF; glucose uptake and metabolism; and erythropoiesis (17, 30, 64). Besides regulating HIF, pVHL is involved in microtubule stabilization and extracellular-matrix fibronectin assembly and other non-HIF-related cellular processes (for a review, see reference 22). While the biology of VHL-associated hemangioblastomas can more easily be attributed to dysregulated HIF, VHL-associated renal carcinogenesis is more complex. Although HIF can modulate RCC metastatic potential through regulation of the chemokine receptor CXCR4 (54) and tumor growth is HIF2 dependent in nude-mouse xenograft models of RCC (27, 28, 65), RCC tumorigenesis most likely requires genetic events in addition to loss of pVHL function (36, 44).

In mice with germ line deficiency for one copy of the murine *VHL* homologue *Vhlh*, the liver seems to be the preferred organ site for vascular-tumor development. In contrast to mice, hepatic vascular tumors are rare manifestations of VHL disease in humans (11, 40, 46). Despite several microscopic features shared with VHL-associated CNS hemangioblastomas, VHL-associated vascular tumors in the murine liver are histogenetically distinct (57). Nevertheless, our model provides a genetic tool to study the role of HIF transcription factors and their individual contributions to the development of VHL-associated vascular tumorigenesis and alterations of gene expression.

Our data suggest that in regard to HIF-regulated gene expression, the level of redundancy among different HIF heterocomplexes is target gene dependent. While the inability to form Hif-1 heterodimers does not affect VHL-mediated angiogenesis or polycythemia, *Pgk*, a gene involved in glycolysis, was significantly reduced with the loss of Hif-1 heterodimers. Consistent with this finding is a report by Hu et al. that demonstrates that in genetically modified 786-0 cells, glycolytic gene expression is preferentially regulated by HIF-1 and not HIF-2 (16). Hepatocytes express the Hif-α homologues Hif-1α, Hif-2α, and Hif-3α (26, 55, 63). Both Hif-1α and Hif-2α form transcriptionally active heterocomplexes in hepatocytes, while the role of Hif-3α, another target for pVHL-mediated proteolysis (39), in hypoxic signaling of hepatocytes is unclear. Based on our studies, Arnt appears to be the only functional Hif-β subunit expressed in hepatocytes, which is consistent with previously published observations (21, 37).

Inactivation of *Vhlh* in hepatocytes results in excessive erythrocytosis from increased Epo production. We have previously shown that serum Epo levels are increased up to 40-fold over normal values (10). Despite the very high hematocrits, we have not observed that PEPCK mutants are prone to thromboembolic complications. Although PEPCK mutants are able to live for at least 15 months, several mice have died at a younger age when exposed to stressful situations. The cause of death in these situations is unclear. Similar observations were made in transgenic mice that express a human *EPO* transgene under the control of the *PDGF-B* chain promoter (59). *EPO* transgenic mice develop similar levels of erythrocytosis and are able to adapt to high hematocrits by increasing eNOS activity, resulting in vasodilatation. Higher blood viscosity from increased erythrocyte flexibility at physiological shear rates appears to be an additional mechanism to prevent cardiovascular complications in these mice (47, 56). Although it has not been formally examined, it is very likely that PEPCK-Cre mutants adapt to erythrocytosis by similar mechanisms. EPO transgenics do not develop liver angiectasis or cavernous hemangiomas (M. Gassmann, personal communication), which makes the involvement of high systemic Epo levels and erythrocytosis in the

development of vascular tumors in PEPCK-Cre mutants unlikely. This notion is supported by the fact that *Vhlh* heterozygotes in which polycythemia is not a clinical feature are still prone to develop vascular tumors in the liver.

It is surprising that the development of erythrocytosis and *Epo* expression in *Vhlh* mutants is not affected by the inability to form functional Hif-1 heterodimers in *Vhlh*/*Hif-1*α double-knockout animals. This finding suggests that Hif-2 is able to fully compensate for the loss of Hif-1 in regard to *Epo* expression in the liver. Based on recently published studies, it has been speculated that the HIF-2 heterodimer may be the more relevant HIF in the transcriptional regulation of *EPO* in experimental retinopathy of prematurity and in human hepatoma and neuroblastoma cell lines (14, 61). By EMSA, we found significant binding of both Hif-1α- and Hif-2α-containing heterocomplexes to the *Epo* HRE in *Vhlh*-deficient liver protein extracts, suggesting that qualitative rather than quantitative differences between Hif-1 and Hif-2 may affect *Epo* expression in the liver. Efforts in our laboratory are under way to determine whether inactivation of *Hif-2*α in contrast to *Hif-1*α deletion will lead to a more significant attenuation of VHL-associated erythrocytosis.

The pharmacological disruption of HIF signaling may be an important therapeutic adjunct for the successful treatment and prevention of VHL-associated vascular tumors that are difficult to manage surgically, such as multifocal CNS hemagioblastomas (for a recent review of clinical management issues, see reference 14). To what degree the different HIF isoforms (HIF-1 versus HIF-2) contribute to the development of specific VHL-associated tumors is still under investigation. Both HIF-1α and HIF-2α are constitutively expressed in RCC (29, 64), where HIF-2 in particular seems to have a tumor-promoting effect even in the presence of wild-type pVHL (27, 28, 35, 65). High levels of HIF-2α have been found in stromal cells (the neoplastic component of VHL hemangioblastomas) (58) and correlate well with *VEGF* mRNA levels, while correlation of HIF-1α expression with tumor *VEGF* levels was less obvious (7). Taken together, these findings and our data suggest that therapeutic intervention strategies aimed at HIF signaling must be designed to efficiently target both HIF homologues. We have shown genetically in mice that inactivation of *Arnt* in a *Vhlh*-deficient background is sufficient to suppress the development of VHL-associated vascular tumors in the liver. Our results should stimulate future investigations into targeting either ARNT directly or its ability to dimerize with HIF-α subunits as a therapeutic strategy in the treatment of VHL vascular tumors.

In summary, our data suggest that in a mouse model of VHL-associated liver hemangiomas, vascular tumorigenesis is mediated by dysregulation of HIF transcription factors. We further propose that different HIF heterocomplexes may play distinct roles in the development of certain clinical features linked to VHL disease.

ACKNOWLEDGMENTS

This work was supported by the Center for Molecular Studies in Digestive and Liver Disease (P30-DK50306) and in part by NIH grants R03-DK062060 and R01-CA100787, as well as seed money from the Department of Medicine, University of Pennsylvania (all to V.H.H.).

We are grateful to the members of the Morphology Core, Center for Molecular Studies in Digestive and Liver Disease (in particular, Gary Swain), for help with the preparation of tissues for histology and image analysis and to Nikita Shrimanker for technical assistance.

REFERENCES

1. **Camenisch, G., R. H. Wenger, and M. Gassmann.** 2002. DNA-binding activity of hypoxia-inducible factors (HIFs). Methods Mol. Biol. **196:**117–129.
2. **Chilov, D., G. Camenisch, I. Kvietikova, U. Ziegler, M. Gassmann, and R. H. Wenger.** 1999. Induction and nuclear translocation of hypoxia-inducible factor-1 (HIF-1): heterodimerization with ARNT is not necessary for nuclear accumulation of HIF-1α. J. Cell Sci. **112:**1203–1212.
3. **Clifford, S. C., M. E. Cockman, A. C. Smallwood, D. R. Mole, E. R. Woodward, P. H. Maxwell, P. J. Ratcliffe, and E. R. Maher.** 2001. Contrasting effects on HIF-1α regulation by disease-causing pVHL mutations correlate with patterns of tumourigenesis in von Hippel-Lindau disease. Hum. Mol. Genet. **10:**1029–1038.
4. **Cohen, D. E., and J. T. Lee.** 2002. X-chromosome inactivation and the search for chromosome-wide silencers. Curr. Opin. Genet. Dev. **12:**219–224.
5. **Da Silva, J. L., C. Lacombe, P. Bruneval, N. Casadevall, M. Leporrier, J. P. Camilleri, J. Bariety, P. Tambourin, and B. Varet.** 1990. Tumor cells are the site of erythropoietin synthesis in human renal cancers associated with polycythemia. Blood **75:**577–582.
6. **Duan, D. R., A. Pause, W. H. Burgess, T. Aso, D. Y. Chen, K. P. Garrett, R. C. Conaway, J. W. Conaway, W. M. Linehan, and R. D. Klausner.** 1995. Inhibition of transcription elongation by the VHL tumor suppressor protein. Science **269:**1402–1406.
7. **Flamme, I., M. Krieg, and K. H. Plate.** 1998. Up-regulation of vascular endothelial growth factor in stromal cells of hemangioblastomas is correlated with up-regulation of the transcription factor HRF/HIF-2α. Am. J. Pathol. **153:**25–29.
8. **Gnarra, J. R., K. Tory, Y. Weng, L. Schmidt, M. H. Wei, H. Li, F. Latif, S. Liu, F. Chen, F. M. Duh, et al.** 1994. Mutations of the VHL tumour suppressor gene in renal carcinoma. Nat. Genet. **7:**85–90.
9. **Gnarra, J. R., J. M. Ward, F. D. Porter, J. R. Wagner, D. E. Devor, A. Grinberg, M. R. Emmert-Buck, H. Westphal, R. D. Klausner, and W. M. Linehan.** 1997. Defective placental vasculogenesis causes embryonic lethality in VHL-deficient mice. Proc. Natl. Acad. Sci. USA **94:**9102–9107.
10. **Haase, V. H., J. N. Glickman, M. Socolovsky, and R. Jaenisch.** 2001. Vascular tumors in livers with targeted inactivation of the von Hippel-Lindau tumor suppressor. Proc. Natl. Acad. Sci. USA **98:**1583–1588.
11. **Hayasaka, K., Y. Tanaka, T. Satoh, and H. Mutoh.** 1999. Hepatic hemangioblastoma: an unusual presentation of von Hippel-Lindau disease. J. Comput. Assist. Tomogr. **23:**565–566.
12. **Hergovich, A., J. Lisztwan, R. Barry, P. Ballschmieter, and W. Krek.** 2003. Regulation of microtubule stability by the von Hippel-Lindau tumour suppressor protein pVHL. Nat. Cell Biol. **5:**64–70.
13. **Herman, J. G., F. Latif, Y. Weng, M. I. Lerman, B. Zbar, S. Liu, D. Samid, D. S. Duan, J. R. Gnarra, W. M. Linehan, et al.** 1994. Silencing of the VHL tumor-suppressor gene by DNA methylation in renal carcinoma. Proc. Natl. Acad. Sci. USA **91:**9700–9704.
14. **Hes, F. J., R. B. van der Luijt, and C. J. Lips.** 2001. Clinical management of Von Hippel-Lindau (VHL) disease. Neth. J. Med. **59:**225–234.
15. **Hoffman, M. A., M. Ohh, H. Yang, J. M. Klco, M. Ivan, and W. G. Kaelin, Jr.** 2001. von Hippel-Lindau protein mutants linked to type 2C VHL disease preserve the ability to downregulate HIF. Hum. Mol. Genet. **10:**1019–1027.
16. **Hu, C. J., L. Y. Wang, L. A. Chodosh, B. Keith, and M. C. Simon.** 2003. Differential roles of hypoxia-inducible factor 1α (HIF-1α) and HIF-2α in hypoxic gene regulation. Mol. Cell. Biol. **23:**9361–9374.
17. **Iliopoulos, O., A. P. Levy, C. Jiang, W. G. Kaelin, Jr., and M. A. Goldberg.** 1996. Negative regulation of hypoxia-inducible genes by the von Hippel-Lindau protein. Proc. Natl. Acad. Sci. USA **93:**10595–10599.
18. **Ivan, M., K. Kondo, H. Yang, W. Kim, J. Valiando, M. Ohh, A. Salic, J. M. Asara, W. S. Lane, and W. G. Kaelin, Jr.** 2001. HIFα targeted for VHL-mediated destruction by proline hydroxylation: implications for O_2 sensing. Science **292:**464–468.
19. **Iwai, K., K. Yamanaka, T. Kamura, N. Minato, R. C. Conaway, J. W. Conaway, R. D. Klausner, and A. Pause.** 1999. Identification of the von Hippel-Lindau tumor-suppressor protein as part of an active E3 ubiquitin ligase complex. Proc. Natl. Acad. Sci. USA **96:**12436–12441.
20. **Jaakkola, P., D. R. Mole, Y. M. Tian, M. I. Wilson, J. Gielbert, S. J. Gaskell, A. Kriegsheim, H. F. Hebestreit, M. Mukherji, C. J. Schofield, P. H. Maxwell, C. W. Pugh, and P. J. Ratcliffe.** 2001. Targeting of HIF-alpha to the von Hippel-Lindau ubiquitylation complex by O_2-regulated prolyl hydroxylation. Science **292:**468–472.
21. **Jain, S., E. Maltepe, M. M. Lu, C. Simon, and C. A. Bradfield.** 1998. Expression of ARNT, ARNT2, HIF1 alpha, HIF2 alpha and Ah receptor mRNAs in the developing mouse. Mech. Dev. **73:**117–123.
22. **Kaelin, W. G., Jr.** 2002. Molecular basis of the VHL hereditary cancer syndrome. Nat. Rev. Cancer **2:**673–682.
23. **Kamura, T., D. M. Koepp, M. N. Conrad, D. Skowyra, R. J. Moreland, O. Iliopoulos, W. S. Lane, W. G. Kaelin, Jr., S. J. Elledge, R. C. Conaway, J. W. Harper, and J. W. Conaway.** 1999. Rbx1, a component of the VHL tumor suppressor complex and SCF ubiquitin ligase. Science **284:**657–661.

24. **Kewley, R. J., M. L. Whitelaw, and A. Chapman-Smith.** 2004. The mammalian basic helix-loop-helix/PAS family of transcriptional regulators. Int. J. Biochem. Cell Biol. **36:**189–204.
25. **Kibel, A., O. Iliopoulos, J. A. DeCaprio, and W. G. Kaelin, Jr.** 1995. Binding of the von Hippel-Lindau tumor suppressor protein to Elongin B and C. Science **269:**1444–1446.
26. **Kietzmann, T., Y. Cornesse, K. Brechtel, S. Modaressi, and K. Jungermann.** 2001. Perivenous expression of the mRNA of the three hypoxia-inducible factor alpha-subunits, HIF1α, HIF2α and HIF3α, in rat liver. Biochem. J. **354:**531–537.
27. **Kondo, K., W. Y. Kim, M. Lechpammer, and W. G. Kaelin, Jr.** 2003. Inhibition of HIF2α is sufficient to suppress pVHL-defective tumor growth. PLoS Biol **1:**E83.
28. **Kondo, K., J. M. Klco, E. Nakamura, M. Lechpammer, and W. G. Kaelin.** 2002. Inhibition of HIF is necessary for tumor suppression by the von Hippel-Lindau protein. Cancer Cell **1:**237–246.
29. **Krieg, M., R. Haas, H. Brauch, T. Acker, I. Flamme, and K. H. Plate.** 2000. Up-regulation of hypoxia-inducible factors HIF-1α and HIF-2α under normoxic conditions in renal carcinoma cells by von Hippel-Lindau tumor suppressor gene loss of function. Oncogene **19:**5435–5443.
30. **Krieg, M., H. H. Marti, and K. H. Plate.** 1998. Coexpression of erythropoietin and vascular endothelial growth factor in nervous system tumors associated with von Hippel-Lindau tumor suppressor gene loss of function. Blood **92:**3388–3393.
31. **Laird, P. W., A. Zijderveld, K. Linders, M. A. Rudnicki, R. Jaenisch, and A. Berns.** 1991. Simplified mammalian DNA isolation procedure. Nucleic Acids Res. **19:**4293.
32. **Ma, W., L. Tessarollo, S. B. Hong, M. Baba, E. Southon, T. C. Back, S. Spence, C. G. Lobe, N. Sharma, G. W. Maher, S. Pack, A. O. Vortmeyer, C. Guo, B. Zbar, and L. S. Schmidt.** 2003. Hepatic vascular tumors, angiectasis in multiple organs, and impaired spermatogenesis in mice with conditional inactivation of the VHL gene. Cancer Res. **63:**5320–5328.
33. **MacGregor, G. R., B. P. Zambrowicz, and P. Soriano.** 1995. Tissue nonspecific alkaline phosphatase is expressed in both embryonic and extraembryonic lineages during mouse embryogenesis but is not required for migration of primordial germ cells. Development **121:**1487–1496.
34. **Maher, E. R., and W. G. Kaelin, Jr.** 1997. von Hippel-Lindau disease. Medicine (Baltimore) **76:**381–391.
35. **Maranchi, J. K., J. R. Vasselli, J. Riss, J. S. Bonifacio, W. M. Linehan, and R. D. Klausner.** 2002. The contribution of VHL substrate binding and HIF-1α to the phenotype of vhl loss in renal cell carcinoma. Cancer Cell **1:**247–253.
36. **Martinez, A., P. Fullwood, K. Kondo, T. Kishida, M. Yao, E. R. Maher, and F. Latif.** 2000. Role of chromosome 3p12-p21 tumour suppressor genes in clear cell renal cell carcinoma: analysis of VHL dependent and VHL independent pathways of tumorigenesis. Mol. Pathol. **53:**137–144.
37. **Maxwell, P. H., G. U. Dachs, J. M. Gleadle, L. G. Nicholls, A. L. Harris, I. J. Stratford, O. Hankinson, C. W. Pugh, and P. J. Ratcliffe.** 1997. Hypoxia-inducible factor-1 modulates gene expression in solid tumors and influences both angiogenesis and tumor growth. Proc. Natl. Acad. Sci. USA **94:**8104–8109.
38. **Maxwell, P. H., M. S. Wiesener, G. W. Chang, S. C. Clifford, E. C. Vaux, M. E. Cockman, C. C. Wykoff, C. W. Pugh, E. R. Maher, and P. J. Ratcliffe.** 1999. The tumour suppressor protein VHL targets hypoxia-inducible factors for oxygen-dependent proteolysis. Nature **399:**271–275.
39. **Maynard, M. A., H. Qi, J. Chung, E. H. Lee, Y. Kondo, S. Hara, R. C. Conaway, J. W. Conaway, and M. Ohh.** 2003. Multiple splice variants of the human HIF-3α locus are targets of the VHL E3 ubiquitin ligase complex. J. Biol. Chem. **21:**21.
40. **McGrath, F. P., R. G. Gibney, D. C. Morris, D. A. Owen, and S. R. Erb.** 1992. Case report: multiple hepatic and pulmonary haemangioblastomas—a new manifestation of von Hippel-Lindau disease. Clin. Radiol. **45:**37–39.
41. **Ohh, M., R. L. Yauch, K. M. Lonergan, J. M. Whaley, A. O. Stemmer-Rachamimov, D. N. Louis, B. J. Gavin, N. Kley, W. G. Kaelin, Jr., and O. Iliopoulos.** 1998. The von Hippel-Lindau tumor suppressor protein is required for proper assembly of an extracellular fibronectin matrix. Mol. Cell **1:**959–968.
42. **Patel, Y. M., J. S. Yun, J. Liu, M. M. McGrane, and R. W. Hanson.** 1994. An analysis of regulatory elements in the phosphoenolpyruvate carboxykinase (GTP) gene which are responsible for its tissue-specific expression and metabolic control in transgenic mice. J. Biol. Chem. **269:**5619–5628.
43. **Pause, A., S. Lee, R. A. Worrell, D. Y. Chen, W. H. Burgess, W. M. Linehan, and R. D. Klausner.** 1997. The von Hippel-Lindau tumor-suppressor gene product forms a stable complex with human CUL-2, a member of the Cdc53 family of proteins. Proc. Natl. Acad. Sci. USA **94:**2156–2161.
44. **Pavlovich, C. P., and L. S. Schmidt.** 2004. Searching for the hereditary causes of renal-cell carcinoma. Nat. Rev. Cancer **4:**381–393.
45. **Postic, C., M. Shiota, K. D. Niswender, T. L. Jetton, Y. Chen, J. M. Moates, K. D. Shelton, J. Lindner, A. D. Cherrington, and M. A. Magnuson.** 1999. Dual roles for glucokinase in glucose homeostasis as determined by liver and pancreatic beta cell-specific gene knock-outs using Cre recombinase. J. Biol. Chem. **274:**305–315.
46. **Rojiani, A. M., D. A. Owen, K. Berry, B. Woodhurst, F. H. Anderson, C. H. Scudamore, and S. Erb.** 1991. Hepatic hemangioblastoma. An unusual presentation in a patient with von Hippel-Lindau disease. Am. J. Surg. Pathol. **15:**81–86.
47. **Ruschitzka, F. T., R. H. Wenger, T. Stallmach, T. Quaschning, C. de Wit, K. Wagner, R. Labugger, M. Kelm, G. Noll, T. Rulicke, S. Shaw, R. L. Lindberg, B. Rodenwaldt, H. Lutz, C. Bauer, T. F. Luscher, and M. Gassmann.** 2000. Nitric oxide prevents cardiovascular disease and determines survival in polyglobulic mice overexpressing erythropoietin. Proc. Natl. Acad. Sci. USA **97:**11609–11613.
48. **Ryan, H. E., M. Poloni, W. McNulty, D. Elson, M. Gassmann, J. M. Arbeit, and R. S. Johnson.** 2000. Hypoxia-inducible factor-1α is a positive factor in solid tumor growth. Cancer Res. **60:**4010–4015.
49. **Scortegagna, M., K. Ding, Y. Oktay, A. Gaur, F. Thurmond, L. J. Yan, B. T. Marck, A. M. Matsumoto, J. M. Shelton, J. A. Richardson, M. J. Bennett, and J. A. Garcia.** 2003. Multiple organ pathology, metabolic abnormalities and impaired homeostasis of reactive oxygen species in Epas1$^{-/-}$ mice. Nat. Genet. **35:**331–340.
50. **Semenza, G. L.** 2001. HIF-1 and mechanisms of hypoxia sensing. Curr. Opin. Cell Biol. **13:**167–171.
51. **Semenza, G. L.** 1999. Regulation of mammalian O_2 homeostasis by hypoxia-inducible factor 1. Annu. Rev. Cell Dev. Biol. **15:**551–578.
52. **Soriano, P.** 1999. Generalized *lacZ* expression with the ROSA26 Cre reporter strain. Nat. Genet. **21:**70–71.
53. **Sowter, H. M., R. R. Raval, J. W. Moore, P. J. Ratcliffe, and A. L. Harris.** 2003. Predominant role of hypoxia-inducible transcription factor (Hif)-1α versus Hif-2α in regulation of the transcriptional response to hypoxia. Cancer Res. **63:**6130–6134.
54. **Staller, P., J. Sulitkova, J. Lisztwan, H. Moch, E. J. Oakeley, and W. Krek.** 2003. Chemokine receptor CXCR4 downregulated by von Hippel-Lindau tumour suppressor pVHL. Nature **425:**307–311.
55. **Stroka, D. M., T. Burkhardt, I. Desbaillets, R. H. Wenger, D. A. Neil, C. Bauer, M. Gassmann, and D. Candinas.** 2001. HIF-1 is expressed in normoxic tissue and displays an organ-specific regulation under systemic hypoxia. FASEB J. **15:**2445–2453.
56. **Vogel, J., I. Kiessling, K. Heinicke, T. Stallmach, P. Ossent, O. Vogel, M. Aulmann, T. Frietsch, H. Schmid-Schonbein, W. Kuschinsky, and M. Gassmann.** 2003. Transgenic mice overexpressing erythropoietin adapt to excessive erythrocytosis by regulating blood viscosity. Blood **102:**2278–2284.
57. **Vortmeyer, A. O., S. Frank, S. Y. Jeong, K. Yuan, B. Ikejiri, Y. S. Lee, D. Bhowmick, R. R. Lonser, R. Smith, G. Rodgers, E. H. Oldfield, and Z. Zhuang.** 2003. Developmental arrest of angioblastic lineage initiates tumorigenesis in von Hippel-Lindau disease. Cancer Res. **63:**7051–7055.
58. **Vortmeyer, A. O., J. R. Gnarra, M. R. Emmert-Buck, D. Katz, W. M. Linehan, E. H. Oldfield, and Z. Zhuang.** 1997. von Hippel-Lindau gene deletion detected in the stromal cell component of a cerebellar hemangioblastoma associated with von Hippel-Lindau disease. Hum. Pathol. **28:**540–543.
59. **Wagner, K. F., D. M. Katschinski, J. Hasegawa, D. Schumacher, B. Meller, U. Gembruch, U. Schramm, W. Jelkmann, M. Gassmann, and J. Fandrey.** 2001. Chronic inborn erythrocytosis leads to cardiac dysfunction and premature death in mice overexpressing erythropoietin. Blood **97:**536–542.
60. **Walisser, J. A., M. K. Bunger, E. Glover, E. B. Harstad, and C. A. Bradfield.** 2004. Patent ductus venosus and dioxin resistance in mice harboring a hypomorphic Arnt allele. J. Biol. Chem. **279:**16326–16331.
61. **Warnecke, C., Z. Zaborowska, J. Kurreck, V. A. Erdmann, U. Frei, M. Wiesener, and K. U. Eckardt.** 2004. Differentiating the functional role of hypoxia-inducible factor (HIF)-1α and HIF-2α (EPAS-1) by the use of RNA interference: erythropoietin is a HIF-2α target gene in Hep3B and Kelly cells. FASEB J. **18:**1462–1464.
62. **Wenger, R. H.** 2002. Cellular adaptation to hypoxia: O_2-sensing protein hydroxylases, hypoxia-inducible transcription factors, and O_2-regulated gene expression. FASEB J. **16:**1151–1162.
63. **Wiesener, M. S., J. S. Jurgensen, C. Rosenberger, C. K. Scholze, J. H. Horstrup, C. Warnecke, S. Mandriota, I. Bechmann, U. A. Frei, C. W. Pugh, P. J. Ratcliffe, S. Bachmann, P. H. Maxwell, and K. U. Eckardt.** 2003. Widespread hypoxia-inducible expression of HIF-2α in distinct cell populations of different organs. FASEB J. **17:**271–273.
64. **Wiesener, M. S., P. M. Munchenhagen, I. Berger, N. V. Morgan, J. Roigas, A. Schwiertz, J. S. Jurgensen, G. Gruber, P. H. Maxwell, S. A. Loning, U. Frei, E. R. Maher, H. J. Grone, and K. U. Eckardt.** 2001. Constitutive activation of hypoxia-inducible genes related to overexpression of hypoxia-inducible factor-1α in clear cell renal carcinomas. Cancer Res. **61:**5215–5222.
65. **Zimmer, M., D. Doucette, N. Siddiqui, and O. Iliopoulos.** 2004. Inhibition of hypoxia-inducible factor is sufficient for growth suppression of VHL$^{-/-}$ tumors. Mol. Cancer Res. **2:**89–95.